Histol Histopathol (2024) 39: 633-646

Histology and Histopathology
From Cell Biology to Tissue Engineering

ORIGINAL ARTICLE Open Access

WTAP enhances the instability of SYTL1 mRNA caused by YTHDF2 in bladder cancer

Jiansong Wang, Jianjun Luo, Xuecheng Wu and Zhuo Li

Department of Urology, Hunan Provincial People's Hospital, The First Affiliated Hospital of Hunan Normal University, Changsha, Hunan, PR China

Summary. Background. Bladder cancer (BCa) is the most frequent type of cancer in humans. The association between m6A modification and the anti-tumor effects of natural killer (NK) cells has been described in BCa. This study intended to investigate the implications of m6A regulators in modulating SYTL1 expression in BCa and the association with the anti-tumor effects of NK cells.

Methods. The prognostic role of SYTL1 in BCa was investigated using bioinformatics analysis, and the correlation between SYTL1 expression and NK cells was analyzed. The effects of SYTL1 on the anti-tumor response of NK-92 cells were examined by RT-qPCR, cytotoxicity, western blot, and ELISA assays. The relationships among WTAP, YTHDF2, and SYTL1 were investigated by RT-qPCR, RIP-qPCR, ELISA, and actinomycin D treatment. Finally, the effects of WTAP and SYTL1 on BCa tumor growth and the anti-tumor response of NK cells were verified *in vivo*.

Results. SYTL1 was reduced in BCa tissues and had a prognostic significance, which was related to NK cell-mediated anti-tumor responses. NK-92 cells produced toxicity to BCa cells, which was further enhanced by SYTL1 overexpression in BCa cells through prompting LDH, NKG2D, NKp30, and NKp44 and IFN-γ levels. WTAP enhanced the degradation of the SYTL1 mRNA by YTHDF2. WTAP and YTHDF2 impaired the anti-tumor response of NK cells in BCa. SYTL1 inhibited the BCa progression in mice while enhancing the anti-tumor response of NK cells.

Conclusions. WTAP inhibited the anti-tumor response of NK cells to BCa cells by promoting the degradation of SYTL1 mRNA through YTHDF2-mediated m6A methylation.

Key words: SYTL1, Natural killer cells, Bladder cancer, WTAP, YTHDF2

Corresponding Author: Zhuo Li, Department of Urology, Hunan Provincial People's Hospital, The First Affiliated Hospital of Hunan Normal University, No.61, Jie Fang Xi Road, Changsha 410005, Hunan, PR China. e-mail: zhuo_L8232@126.com

www.hh.um.es. DOI: 10.14670/HH-18-671

Introduction

Bladder cancer (BCa) occurs in the epithelial lining of the urinary bladder and is among the most common kinds of cancer in humans, killing thousands of people annually (Martinez Rodriguez et al., 2017). Until recently, treatment for BCa has seen little progress, and clinicians were stuck with a limited range of therapeutics to offer patients for three decades (Grayson, 2017). The current standard of care is neoadjuvant chemotherapy followed by radical cystectomy, which could contribute to significant morbidities, while modifications in the chemotherapy regimens, as well as in perioperative care and surgical approach, have led to better overall toxicity profile and faster recovery (Ghandour et al., 2019). Thus, it is necessary to identify novel prognostic markers and candidate targets for BCa to enhance the toxicity profile.

According to the latest report, the risk score prognostic system was constructed from The Cancer Genome Atlas and Gene Expression Omnibus database with the aid of bioinformatics tools, and five genes were filtered and found to be correlated with the tumor grade and overall survival in muscle-invasive BCa, in which synaptotagmin-like protein 1 (SYTL1) showed the closest relationship (Xu et al., 2021). SYTL1 (also named SLP1) belongs to the synaptotagmin-like protein family of secretory factors characterized by a Rab-binding domain at the N-terminal and two tandem-C2 domains at the C-terminal (Meijuan et al., 2023). However, the upstream regulatory mechanism of SYTL1 in BCa remains quite unknown. N6-methyladenosine (m6A), a methylation modification that occurs in the N6-position of adenosine, is installed by m6A methyltransferases, removed by m6A demethylases and recognized by reader proteins, which regulate RNA metabolism, including translation, degradation and microRNA processing (He et al., 2019). Wilms tumor 1-associated protein (WTAP), one of the m6A methyltransferases, plays an important part in the occurrence and development of BCa and can be regarded as a possible target for BCa treatment, offering a new

basis for clinical diagnoses (Chen and Wang, 2018). Furthermore, the levels of m6A regulators have been revealed to be correlated with the expression of immunoregulators and immune infiltration levels in esophageal cancer (Zhao et al., 2021). NK cells are powerful malignant cells, providing rapid immune responses via direct cytotoxicity without the need for antigen presentation, and play an essential role in preventing early tumor growth and metastasis (Lian et al., 2021). Therefore, we posited that the SYTL1 downregulation was regulated by WTAP in BCa, which might be related to the dysfunction of NK cells. Here, we aimed to explore the biological roles and potential mechanisms of SYTL1 in the toxic effects of NK cells. These findings may provide a basic rationale for new approaches in developing antitumor therapeutics for BCa.

Materials and methods

Bioinformatics prediction

The Kaplan-Meier Plotter database (http://kmplot.com/analysis/) assesses the correlation between the expression of all genes (mRNA, microRNA, protein) and patients' survival in more than 30,000 samples from 21 tumor types. The Kaplan-Meier Plotter database was used here to analyze the correlation between SYTL1 in BCa and patients' prognosis. The GEPIA database (http://gepia.cancer-pku.cn/index.html) analyzes RNA sequencing expression data from 9,736 tumors and 8,587 normal samples from the TCGA and GTEx programs. In this study, the GEPIA database was used to customize the correlation between SYTL1 expression and METTL3, WTAP, and YTHDF2 expression in BCa tissues.

Collection of tumor tissues

The study was approved by the Ethics Committee of Hunan Provincial People's Hospital, and informed consent was signed by all patients. From May 2018 to April 2020, a total of 35 BCa tissue samples as well as paracancerous tissue were collected at Hunan Provincial People's Hospital. All patients were diagnosed with BCa histopathologically and underwent radical cystectomy. The studies abide by the *Declaration of Helsinki* principles.

Cell culture

An immortalized human uroepithelial cell line (SV-HUC-1) and NK-92 cells were purchased from American Type Culture Collection (Manassas, VA, USA). BCa cell lines 5637, T24, SW780, and J82 were purchased from the National Collection of Authenticated Cell Cultures (Shanghai, China). SV-HUC-1, T24, and SW780 cells were cultured in DMEM (A4192101, Gibco, Carlsbad, CA, USA) spiked with 10% FBS. BCa cell lines 5637 and J82 were cultured in RPMI-1640 (12633020, Gibco) containing 10% FBS. NK-92 cells were cultured in alpha-minimum essential medium (41061029, Gibco) supplemented with 20% FBS and 100 U/mL IL-2. All media were spiked with 1% penicillin and streptomycin, and the culture environment was 5% CO_2 and 37°C.

Lentivirus infection

Cells with artificial upregulation or downregulation of WTAP, YTHDF2, and SYTL1 were generated via lentiviral infection. All lentiviruses were purchased from Shanghai GenePharma Co., Ltd. (Shanghai, China). When the cell confluence reached 40-60%, the 5637 and SW780 cells were infected with different types of lentiviruses according to the instructions, respectively. The lentiviral vector was replaced with fresh medium 24h after infection. After 48h, the puromycin-positive cells were screened out, and the expression was detected using RT-qPCR after screening the stably expressed cells.

RT-qPCR assay

The collected tissues or cells to be tested were extracted with TRIzol (15596026, Invitrogen Inc., Carlsbad, CA, USA) according to the manufacturer's procedure, and then DNase I enzyme was added to eliminate the effect of DNA. The concentration and purity of RNA were determined by UV-Vis spectrophotometer UV7 (30254726, Mettler Toledo, Shanghai, China). RNA was then reverse transcribed into cDNA using a Promega M-MLV kit (M1701, Promega Corporation, Madison, WI, USA). Finally, qPCR was performed using SYBR Select Master Mix (Applied Biosystems, Inc., Foster City, CA, USA) on an Applied Biosystems 7500 Fast system (4365464, Applied Biosystems). For analyses, the expression of target genes was normalized to that of the housekeeping gene glyceraldehyde-3-phosphate dehydrogenase (GAPDH). Relative expression was determined by the $2^{-\Delta\Delta CT}$ method (Livak and Schmittgen, 2001). cDNA fragments were amplified using the gene-specific primers provided in Table 1.

Co-culture of NK cells with BCa cells

Briefly, treated 5637 or SW780 cells were seeded into 96-well plates at a density of 10^4 per well, and the activated NK-92 cells stimulated with IL-2 were seeded at an E:T ratio of 10:1. After a 6-h incubation at 37°C in 5% CO_2, the supernatant was collected to detect the cytotoxicity and IFN-γ content in the supernatant. The cells were collected to detect the NKG2D receptor activation.

Cytotoxicity assay

The lactate dehydrogenase (LDH) content in the

supernatant of the co-culture system was measured using the LDH Cytotoxicity Assay Kit (C0016, Beyotime) according to the manufacturer's procedure. LDH assay working solution (60 μL) was supplemented to the supernatant according to the kit requirements and incubated for 0.5h at room temperature in the dark. The absorbance at 490 nm was directly measured using a Multiskan™ FC microplate reader (51119180ET, Thermo Fisher Scientific Inc., Waltham, MA, USA).

Enzyme-linked immunosorbent (ELISA) assays

We used the human IFN-γ ELISA Kit (DIF50C, R&D Systems, Minneapolis, MN, USA) to detect the level of IFN-γ in the co-culture chamber. The supernatant (50 μL) was added to the 96-well plate, followed by the addition of 50 μL diluted antibody capture solution and detection antibody mixture. The plate was sealed and incubated at room temperature for 60 min. After the incubation with 100 μL tetramethylbenzidine developing solution for 10 min in the dark and the termination with 100 μL termination solution, the absorbance at 450 nm was read with the microplate reader, which was converted to the final content according to the standard curve.

Western blot

Cells or tissues to be tested were lysed with 3 mL RIPA lysis buffer (R0010, Beijing Solarbio Life Sciences Co., Ltd., Beijing, China) and centrifuged at 3000 g for 30 min. The supernatant was separated, and the protein concentration was quantified using the bicinchoninic acid assay protein concentration assay kit (P0010S, Beyotime). After sodium dodecyl sulfate-polyacrylamide gel electrophoresis, the separated proteins were electrotransferred onto the polyvinylidene fluoride (PVDF) membrane. The membrane was incubated with 5% BSA for 1h at room temperature and incubated with the diluted primary antibodies to NKG2D (1:1000, PA5-79570, Thermo Fisher), Anti-NKp30 (1:1000, ab186425, Abcam, Cambridge, UK), NKp44 (1:250, MAB2249, Novus Biological Inc., Littleton, CO, USA), and GAPDH (1:2500, ab9485, Abcam) overnight at 4°C and with HRP-coupled secondary antibody goat anti-rabbit IgG H&L (1:2000, ab6721, Abcam) or goat anti-mouse IgG H&L (1:5000, 31430, Thermo Fisher) at room temperature for 1h. The membrane was developed using an enhanced ECL chemiluminescence detection kit (36222ES60, Yeasen), and the protein blots were photographed and analyzed for grayscale values using Image J.

Detection of m6A methylation modifications

The m6A methylation levels were quantified in 5637 and SW780 cells using the m6A RNA Methylation Assay Kit (ab185912, Abcam) according to the manufacturer's procedure. After extraction of total RNA from cells using TRIeasy™ Total RNA Extraction Reagent, 200 ng of RNA samples were added to a 96-well plate, and 80 μL diluted binding solution was added to each well for a 90-min incubation at 37°C. After that, the samples in each well were incubated with 50 μL diluted antibody capture solution for 1h and with 50 μL diluted m6A antibody for 30 min, and finally with 50 μL diluted enhancer solution for 30 min (all at room temperature). The color development reaction was carried out by adding the developing solution for 1 min, and finally, the absorbance was read at 450 nm with the microplate reader to determine the relative m6A methylation in the RNA samples.

RNA immunoprecipitation (RIP) assay

According to the instructions of the RIP kit (P0101, Geneseed, Guangzhou, Guangdong, China), RIP was conducted. The cells were lysed using cell lysis solution and centrifuged at 14000 g for 10 min at 4°C, and the supernatant was collected. Magnetic beads coupled with YTHDF2 antibody (ab220163, Abcam), WTAP (ab195380, Abcam), or recombinant rabbit IgG antibody [EPR25A]-isotype control (ab172730, Abcam) were added to the supernatant and incubated at 4°C overnight. The beads were washed with immunoprecipitation lysis buffer and collected by centrifugation at 300 g for 5 min. The eluent was used to elute the complexes bound to the magnetic beads. After RNA extraction using TRIeasy™ Total RNA Extraction Reagent, the RNA was reverse transcribed into cDNA using reverse transcriptase and finally subjected to qPCR analysis.

m6A-immunoprecipitation-qPCR

We quantified the m6A methylation modification on

Table 1. Primers used in this study.

Gene	Forward Sequence (5'-3')	Reverse Sequence (5'-3')
SYTL1	GGCGGTGAAGAAACGGAATCTG	AGATGTTGCGACCCAGGCTTTC
WTAP	GCAACAACAGCAGGAGTCTGCA	CTGCTGGACTTGCTTGAGGTAC
YTHDF2	TAGCCAGCTACAAGCACACCAC	CAACCGTTGCTGCAGTCTGTGT
GAPDH	GTCTCCTCTGACTTCAACAGCG	ACCACCCTGTTGCTGTAGCCAA

SYTL1, Synaptotagmin-like protein 1; WTAP, Wilms tumor 1-associated protein; YTHDF2, YTH domain-containing family protein 2; GAPDH, glyceraldehyde-3-phosphate dehydrogenase.

SYTL1 mRNA using the Pierce™ Classic Magnetic Beads IP Kit (88804, Thermo Fisher) according to the procedure. The cells to be tested were dissociated into single-cell suspensions, lysed with cell lysis solution, and centrifuged at 14000 g for 10 min at 4°C. The precipitate was removed, and the supernatant was harvested. Magnetic beads coupled with anti-m6A (ab208577, Abcam) were added to the supernatant and incubated overnight at 4°C. The beads were centrifuged with the immunoprecipitation complex at 300 g for 5 min, followed by elution of the RNA complex using the elution buffer. The RNA was extracted and then reverse transcribed, and SYTL1 mRNA in total RNA was measured using qPCR.

The half-life of SYTL1 mRNA

After incubation of 5637 cells and SW780 cells with Actinomycetes D (2 mg/mL, SBR00013, Sigma-Aldrich Chemical Company, St Louis, MO, USA) for 0h, 6h, and 12h, the cells were subjected to total RNA extraction. The level of SYTL1 mRNA was detected by RT-qPCR to verify the effect of YTHDF2 on the stability of SYTL1 mRNA.

Animal experiments

All animals were manipulated according to institutional guidelines and the permission granted by Hunan Provincial People's Hospital. The mixture of 5637 or SW780 cells (5×10^6 cell/100 μL) with 30% Matrigel was subcutaneously injected into specific-pathogen-free BALB/c mice (4-5 weeks, ~20 g, male, Beijing Vital River Laboratory Animal Technology Co., Ltd., Beijing, China) to establish a xenograft model. SW780 cells infected with oe-SYTL1 or control lentivirus (oe-NC) and 5637 cells infected with oe-WTAP or control lentivirus (oe-NC), oe-WTAP + sh-YTHDF2 or oe-WTAP + sh-NC were used for injection (n=6 for each group). Tumor volume was recorded at an interval of 5 days using a caliper and calculated as the formula: $V=(\text{width}^2\times\text{length}\times0.5)$. Nude mice were euthanized by injection of pentobarbital sodium (100 mg/kg) on day 35 of the experiment, and tumor tissues were removed and weighed. A portion of tumor tissues was made into paraffin tissue sections for subsequent experiments, and another portion was used for single-cell isolation.

Cell isolation from tumor tissues

The tumor tissues were cut into pieces of about 1 mm^3 and incubated in serum-free DMEM with 0.25 mg/mL Dnase I as well as 1.65 mg/mL type IV collagenase in a shaker for 1h at room temperature. At the end of incubation, centrifugation was performed at 400 g for 5 min, and the supernatant was discarded. The single-cell suspension was filtered through a 70 μm filter, and the isolated cells were transferred to fresh DMEM medium with 10% FBS as well as 1% penicillin-streptomycin for flow cytometry.

Flow cytometry

The isolated cells from the tissues were collected into flow tubes, and centrifuged at 500 g for 5 min. After that, 10^6 cells were resuspended into 100 μL phosphate-buffered saline and incubated with allophycocyanin-labeled NK1.1 monoclonal antibody (1:300, 17-5941-82, Thermo Fisher), and fluorescein isothiocyanate-labeled CD3 monoclonal antibody (1:200, 11-0032-82, Thermo Fisher) for 30 min at room temperature in the dark. The cells were then fixed in paraformaldehyde and loaded onto an Attune™ NxT flow cytometer (A24860, Thermo Fisher). The data were analyzed with FlowJo software.

Immunohistochemistry

The tumor tissues were fixed with 4% tissue cell fixative, embedded in paraffin, and made into 4-μm sections. Paraffin-embedded tissue sections (4 μm) to be tested were dewaxed in xylene and then rehydrated using different concentrations (100%, 100%, 95%, 90%, 80%, 70%) of ethanol. The sections were immersed in sodium citrate buffer for antigen retrieval, and then endogenous peroxidase inactivation was performed with 3% hydrogen peroxide. Non-specific binding sites were sealed using 5% BSA for 15 min, after which the sections were incubated overnight at 4°C with diluted specific antibodies. The sections were incubated with the corresponding HRP-coupled goat anti-rabbit IgG (H+L) secondary antibody (1:10,000, 31460, Thermo Fisher) at room temperature for 40 min and stained using 3,3′-diaminobenzidine (D8001, Sigma-Aldrich). The nuclei were then counter-stained with hematoxylin, and after sealing with neutral gum, the sections were finally photographed under a light microscope. The following primary antibodies were used: WTAP (1:1000, ab195380, Abcam), SYTL1 (1:500, PA5-58126, Thermo Fisher), YTHDF2 (1:100, PA5-100053, Thermo Fisher), and IFN-γ (1:500, PA5-95560, Thermo Fisher). The intensity of immunostaining was scored on a 4-point scale: 0 for negative, 1 for weak staining intensity, 2 for moderate staining intensity, and 3 for strong staining intensity, and the grayscale values of the staining intensity of immunohistochemistry were analyzed using Image J software. The final positive staining score was derived from the total score based on the product of the proportion of the area of each staining intensity of the section and the corresponding score.

Statistical information

Statistical significance was determined using Prism 8.0 (GraphPad, San Diego, CA, USA). The error bars in bar graphs represented the mean ± standard deviation (SD). The differences between any two independent groups were analyzed using the unpaired or paired *t*-test.

One-way or two-way analysis of variance (ANOVA) was used to determine significance across multiple groups. $p<0.05$ was considered significant. All experiments were performed in triplicate.

Results

The prognostic significance of SYTL1 in BCa is related to the anti-tumor response of NK cells

SYTL1 has been reported as a prognostic biomarker for BCa, and its expression was negatively correlated with the tumor stage (Xu et al., 2021). By Kaplan-Meier Plotter (http://kmplot.com/analysis/index.php?p=service), we learned that SYTL1 had a prognostic significance in BCa and that high expression of SYTL1 was associated with higher survival of patients (Fig. 1A). We performed an RT-qPCR assay of SYTL1 expression in the collected 35 BCa tissues and their paracancerous tissues. It was found that SYTL1 was poorly expressed in BCa tissues (Fig. 1B). We then performed restrict analysis based on cellular content in Kaplan-Meier Plotter to dissect the relevance of SYTL1 to immune cells. The prognostic significance of SYTL1 was still observed in patients with decreased $CD4^+$ memory T-cells, decreased $CD8^+$ T-cells, and decreased macrophages, demonstrating that the prognostic significance of SYTL1 was independent of the three immune cells (Fig. 1C). However, we observed no significant prognostic effect of SYTL1 in NK cells decreased patients, suggesting that the prognostic significance of SYTL1 in cancer was related to NK cells (Fig. 1D).

We then examined the expression of SYTL1 in the immortalized human uroepithelial cell line SV-HUC-1 and BCa cell lines 5637, T24, SW780, and J82, and found that SYTL1 was poorly expressed in BCa cell lines (Fig. 1E). We selected 5637 and SW780, which were often used as subjects, as the cell lines used in subsequent experiments. We treated 5637 cells and SW780 cells with sh-SYTL1 or oe-SYTL1 and detected the expression by RT-qPCR (Fig. 1F).

The two cell lines were subsequently co-cultured with NK-92 cells, and the LDH cytotoxicity assay was performed on the supernatant. It was found that the LDH content in the supernatant was reduced and the cytotoxicity was attenuated after the silencing of SYTL1 (Fig. 1G). Similarly, we performed ELISA on the supernatant to detect the levels of IFN-γ, and the release of IFN-γ from NK cells was reduced after silencing of SYTL1 on 5637 and SW780 cells (Fig. 1H). Western blot assay revealed a significant decrease in NKG2D receptor activation (Fig. 1I). These results indicated that silencing of SYTL1 increased the resistance of 5637 and SW780 cells to the anti-tumor response of NK-92 cells. In contrast, overexpression of SYTL1 promoted the killing effects on 5637 and SW780 cells by NK-92 cells, with increased LDH content detected in the supernatant (Fig. 1G), increased cytotoxicity, and upregulated expression of IFN-γ as well as NKG2D (Fig. 1H,I). We further analyzed the expression of activation markers NKp30 and NKp44 in NK cells using western blot and showed that upregulation of SYTL1 induced an increase in the expression of both, while downregulation of SYTL1 inhibited the activation of NKp30 and NKp44 instead (Fig. 1J). It was thus preliminarily confirmed that SYTL1 overexpression in BCa cells promoted NK cell-mediated anti-tumor responses.

WTAP suppresses SYTL1 expression through m6A methylation modification

Analysis of the correlation between the expression of common writers responsible for m6A modification and SYTL1 expression in GEPIA (http://gepia.cancer-pku.cn/index.html) revealed that WTAP was significantly correlated with SYTL1 expression (Fig. 2A), while it was not significantly correlated with METTL3 expression (Fig. 2B). We performed RT-qPCR of WTAP in collected BCa tissue samples and paracancerous tissues. WTAP was overexpressed in BCa tissues, and there was a negative correlation between WTAP and SYTL1 expression in BCa tissues (Fig. 2C). Consistently, WTAP expression was upregulated in the BCa cell lines relative to the immortalized human uroepithelial cell line SV-HUC-1 (Fig. 2D). Subsequent assays for m6A methylation levels revealed that the level of m6A modification was higher in BCa cell lines than in SV-HUC-1 cells (Fig. 2E).

We then silenced WTAP and overexpressed WTAP in 5637 and SW780 cells (Fig. 2F). First, the binding relationship between WTAP and SYTL1 mRNA was verified by RIP-qPCR. SYTL1 mRNA expression was increased in the complex pulled down by anti-WTAP. SYTL1 mRNA expression was decreased in the complex with WTAP knockdown, which was enhanced in the complex with WTAP overexpression, indicating that there was a binding relationship between WTAP and SYTL1 mRNA (Fig. 2G). The m6A methylation levels in RNA were then examined and found to be significantly elevated in 5637 and SW780 cells overexpressing WTAP, whereas m6A methylation levels were suppressed in SW780 and SW780 cells silenced with WTAP (Fig. 2H). Subsequently, the expression of SYTL1 was examined in these two cell lines using RT-qPCR. The results showed that SYTL1 was upregulated after silencing of WTAP, whereas overexpression of WTAP suppressed the expression of SYTL1 (Fig. 2I). We then performed m6A-IP-qPCR to investigate the level of m6A methylation modification on SYTL1 mRNA. As expected, silencing of WTAP decreased the level of m6A methylation modification on SYTL1, whereas overexpression of WTAP promoted m6A methylation modification on SYTL1 mRNA (Fig. 2J). It indicates that WTAP suppresses SYTL1 expression through m6A methylation modification.

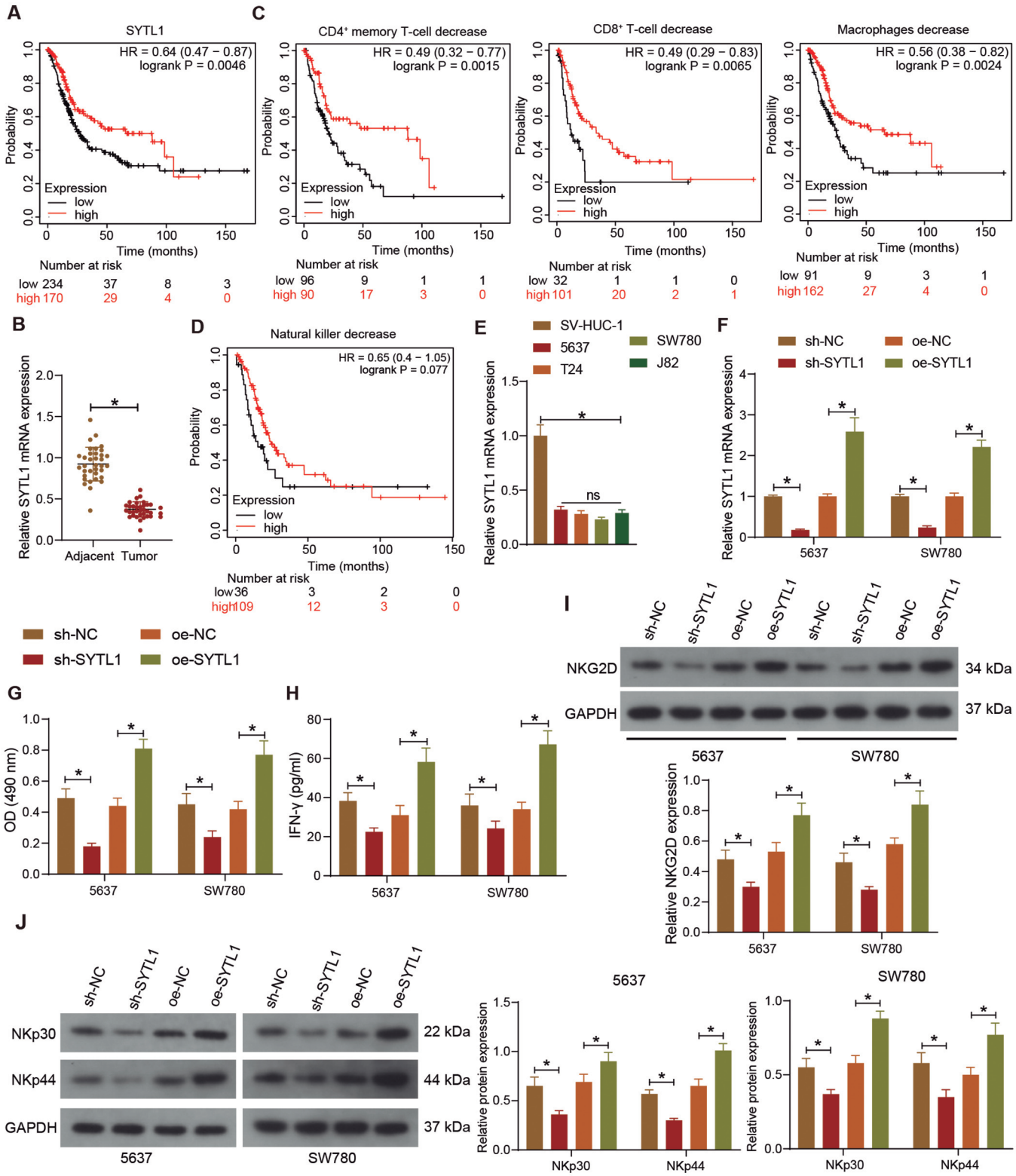

Fig. 1. Prognostic significance of SYTL1 in BCa is related to the anti-tumor response of NK cells. **A.** Analysis of the prognostic significance of SYTL1 expression in BCa. **B.** Detection of SYTL1 expression in BCa tissues and paracancerous tissues by RT-qPCR (n=35). **C.** The correlation between SYTL1 expression and CD4$^+$ memory T-cell, CD8$^+$ T-cell, and macrophage reduction in BCa. **D.** The correlation between SYTL1 expression and NK cell reduction in BCa. **E.** Expression of SYTL1 in SV-HUC-1 cells and BCa cell lines detected by RT-qPCR. **F.** RT-qPCR detection of SYTL1 expression in 5637 and SW780 cells with silencing and overexpressing SYTL1. **G.** LDH content in the supernatant of the co-culture system. **H.** The determination of IFN-γ levels in the supernatant of the co-culture system was measured using ELISA. **I.** NKG2D expression in the co-culture system was measured using western blot assays. **J.** NKp30 and NKp44 expression in the co-culture system was measured using western blot assays. Data are the mean ± SD (paired t-test (B), one-way (E), or two-way ANOVA (F, G, H, I, J)). Data represent at least three independent experiments. *p<0.05.

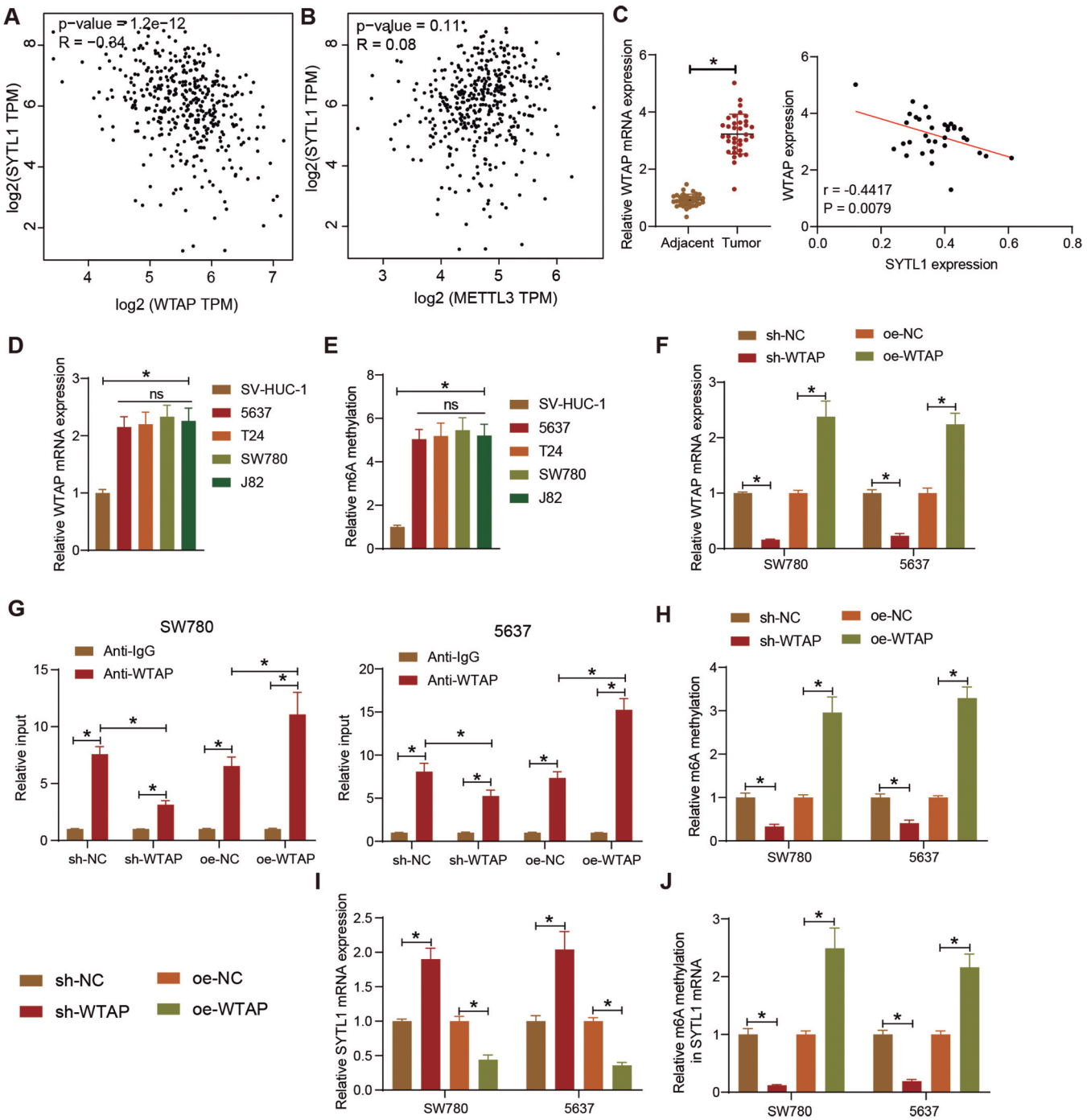

Fig. 2. WTAP suppresses SYTL1 expression through m6A methylation modification. **A.** The correlation analysis between SYTL1 and WTAP expression in BCa. **B.** The correlation analysis between SYTL1 and METTL3 expression in BCa. **C.** WTAP expression in BCa tissues and paracancerous tissues by RT-qPCR and the Person's correlation analysis between SYTL1 and WTAP in BCa tissues. **D.** WTAP expression in SV-HUC-1 cells and BCa cell lines by RT-qPCR. **E.** m6A methylation in SV-HUC-1 cells and BCa cell lines. **F.** RT-qPCR detection of WTAP expression in SW780 and 5637 cells overexpressing and silencing of WTAP. **G.** The binding relationship between WTAP and SYTL1 mRNA by RIP-qPCR. **H.** m6A methylation in SW780 and 5637 cells overexpressing or silencing of WTAP. **I.** RT-qPCR detection of SYTL1 expression in SW780 and 5637 cells overexpressing and silencing of WTAP. **J.** SYTL1 mRNA m6A methylation levels in SW780 and 5637 cells overexpressing and silencing of WTAP by m6A-IP-qPCR. Data are the mean ± SD (paired t-test (C), one-way (D, E), or two-way ANOVA (F, G, H, I, J)). Data represent at least three independent experiments. *p<0.05.

WTAP enhances the degradation of SYTL1 mRNA by YTHDF2-mediated m6A modification

The m6A reader YTHDF2, which promotes mRNA decay through the AGO2 system, was significantly and negatively correlated with the expression of SYTL1, as demonstrated by the GEPIA website (Fig. 3A). We therefore speculated that WTAP modulates SYTL1 mRNA by m6A modification, followed by YTHDF2 recognition, leading to the degradation of SYTL1 mRNA. We next tested this conjecture via a series of assays. First, we treated 5637 and SW780 cells with lentiviruses harboring overexpression or silencing of YTHDF2 and assayed the mRNA expression of YTHDF2 to verify the infection efficiency (Fig. 3B). The expression of SYTL1 mRNA was then detected by RT-qPCR. SYTL1 mRNA expression was upregulated in the complex with sh-YTHDF2, whereas SYTL1 mRNA expression was significantly decreased in the complex with oe-YTHDF2 (Fig. 3C). The binding relationship between YTHDF2 and SYTL1 mRNA was examined by RIP-qPCR (Fig. 3D). The results showed that the SYTL1 mRNA expression was higher in the anti-YTHDF2 group compared to the anti-IgG group. SYTL1

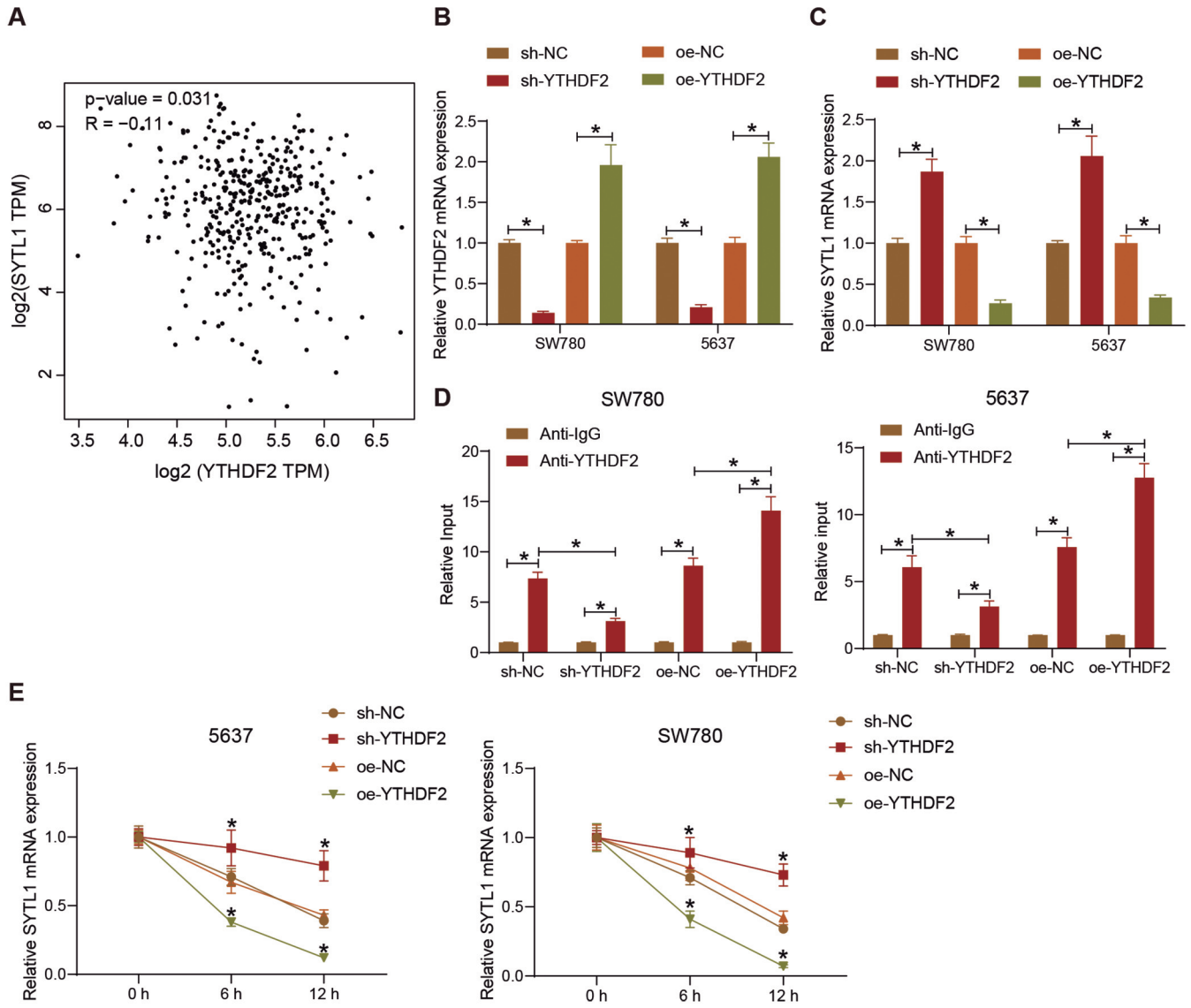

Fig. 3. WTAP enhances the degradation of SYTL1 mRNA via YTHDF2. **A.** The correlation analysis between SYTL1 and YTHDF2 expression in BCa. SW780 and 5637 cells were infected with lentiviruses harboring sh-YTHDF2 or oe-YTHDF2. **B.** RT-qPCR detection of YTHDF2 expression in SW780 and 5637 cells. **C.** RT-qPCR detection of SYTL1 expression in SW780 and 5637 cells. **D.** The binding relationship between YTHDF2 and SYTL1 mRNA was measured using RIP-qPCR. **E.** The effect of YTHDF2 on SYTL1 mRNA stability was analyzed using actinomycin D treatment. Data are the mean ± SD (two-way ANOVA). Data represent at least three independent experiments. *$p<0.05$.

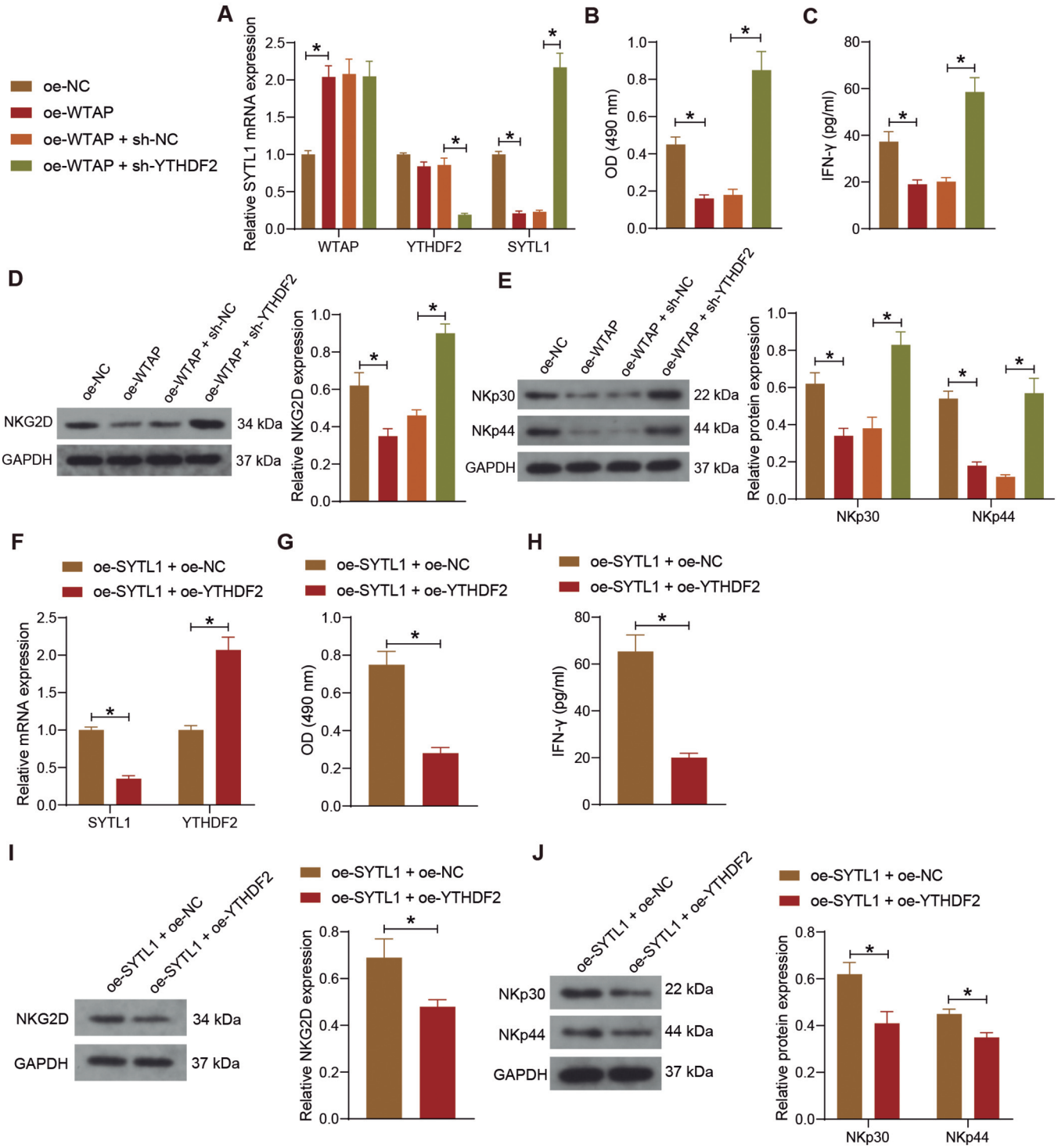

Fig. 4. WTAP and YTHDF2 overexpression in BCa cells mitigate the anti-tumor response of NK cells *in vitro*. 5637 cells infected with oe-WTAP alone or with sh-YTHDF2 (oe-NC or oe-WTAP + sh-NC as controls) were co-cultured with NK cells. **A.** WTAP, YTHDF2, and SYTL1 expression by RT-qPCR. **B.** LDH content in the supernatant of the co-culture system. **C.** The determination of IFN-γ levels in the supernatant of the co-culture system was measured using ELISA. **D.** NKG2D protein expression in the co-culture system was measured using western blot assays. **E.** NKp30 and NKp44 protein expression in the co-culture system were measured using western blot assays. SW780 cells infected with oe-SYTL1 + oe-YTHDF2 (oe-SYTL1 + oe-NC as controls) were co-cultured with NK cells. **F.** YTHDF2 and SYTL1 expression by RT-qPCR. **G.** LDH content in the supernatant of the co-culture system. **H.** The determination of IFN-γ levels in the supernatant of the co-culture system was measured using ELISA. **I.** NKG2D expression in the co-culture system was measured using western blot assays. **J.** NKp30 and NKp44 protein expression in the co-culture system were measured using western blot assays. Data are the mean ± SD (unpaired t-test (G, H, I), one-way (B, C, D), or two-way ANOVA (A, E, F)). Data represent at least three independent experiments. *$p<0.05$.

mRNA expression was reduced in 5637 and SW780 cells after silencing of YTHDF2, while the opposite trends were observed in cells overexpressing YTHDF2. We then examined SYTL1 mRNA levels in 5637 and SW780 cells at different periods after treatment with the transcriptional inhibitor actinomycin D. SYTL1 mRNA expression was reduced after actinomycin D treatment. Moreover, overexpression of YTHDF2 accelerated this process, while silencing of YTHDF2 delayed the process (Fig. 3E). It indicates that the recognition of SYTL1 mRNA by YTHDF2 decreases the stability of mRNA, thus leading to mRNA degradation.

WTAP and YTHDF2 overexpression in BCa cells mitigates the anti-tumor effects of NK cells

We next investigated the effect of WTAP overexpression on the anti-tumor response of BC cells to NK cells. We co-cultured 5637 cells overexpressing WTAP or overexpressing WTAP and silencing YTHDF2 with NK-92 cells. The supernatant was collected for a series of assays. There was no significant change in YTHDF2 mRNA expression, and SYTL1 mRNA expression was inhibited after overexpression of WATP (Fig. 4A). The decreased level of LDH in the co-culture system (Fig. 4B) indicated reduced cytotoxicity. Meanwhile, the lowered level of IFN-γ (Fig. 4C) and the decreased expression of NKG2D, NKp30, and NKp44 (Fig. 4D,E) indicated that the killing effect of NK-92 cells on BCa cells was diminished. In contrast, overexpression of WTAP followed by silencing of YTHDF2 resulted in significant restoration of SYTL1 expression (Fig. 4A), increased LDH levels in the co-culture system (Fig. 4B), and upregulation of IFN-γ levels (Fig. 4C) and NKG2D, NKp30, and NKp44 protein expression (Fig. 4D,E), signifying that silencing of YTHDF2 reverses the attenuating effects of WTAP on NK cells.

To further validate the effects of YTHDF2 on SYTL1, we treated SW780 cells with overexpression of

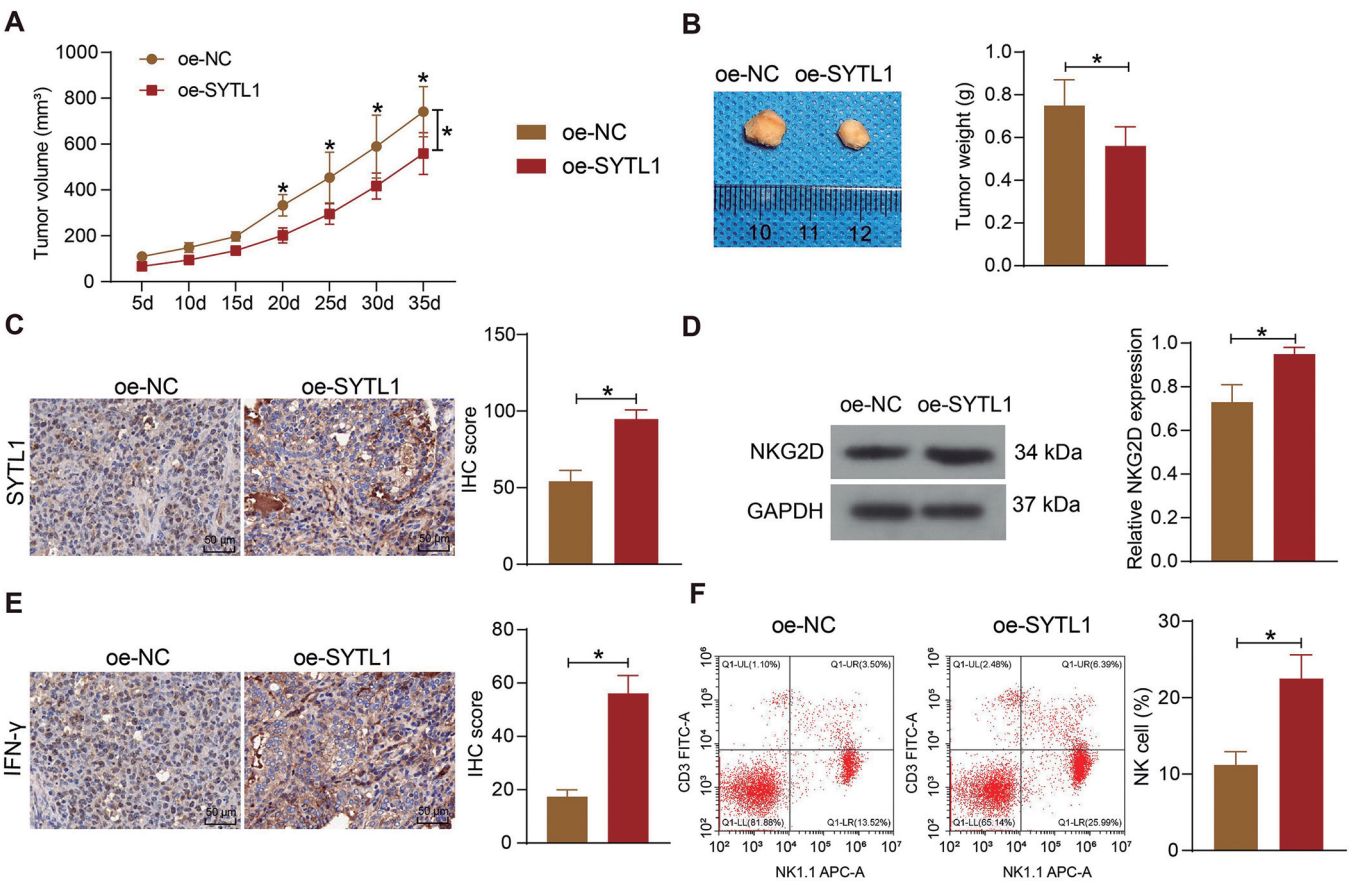

Fig. 5. Overexpression of SYTL1 inhibits BCa tumor growth and promotes NK cell-mediated anti-tumor responses in mice. SW780 cells overexpressing SYTL1 were injected into nude mice. **A.** The curve of tumor volume within 35 days. **B.** Representative xenografts and tumor weight detection. **C.** Immunohistochemical detection of SYTL1 expression in tumor tissues from mice. **D.** NKG2D expression in tumor tissues from mice was measured using western blot assays. **E.** Immunohistochemical detection of IFN-γ expression in tumor tissues from mice. **F.** Flow cytometric detection of NK cells in single cell suspensions isolated from tumor tissues from mice. Data are the mean ± SD (unpaired t-test (B, C, D, E, F) or two-way ANOVA (A)). n=6 for each group. *p<0.05.

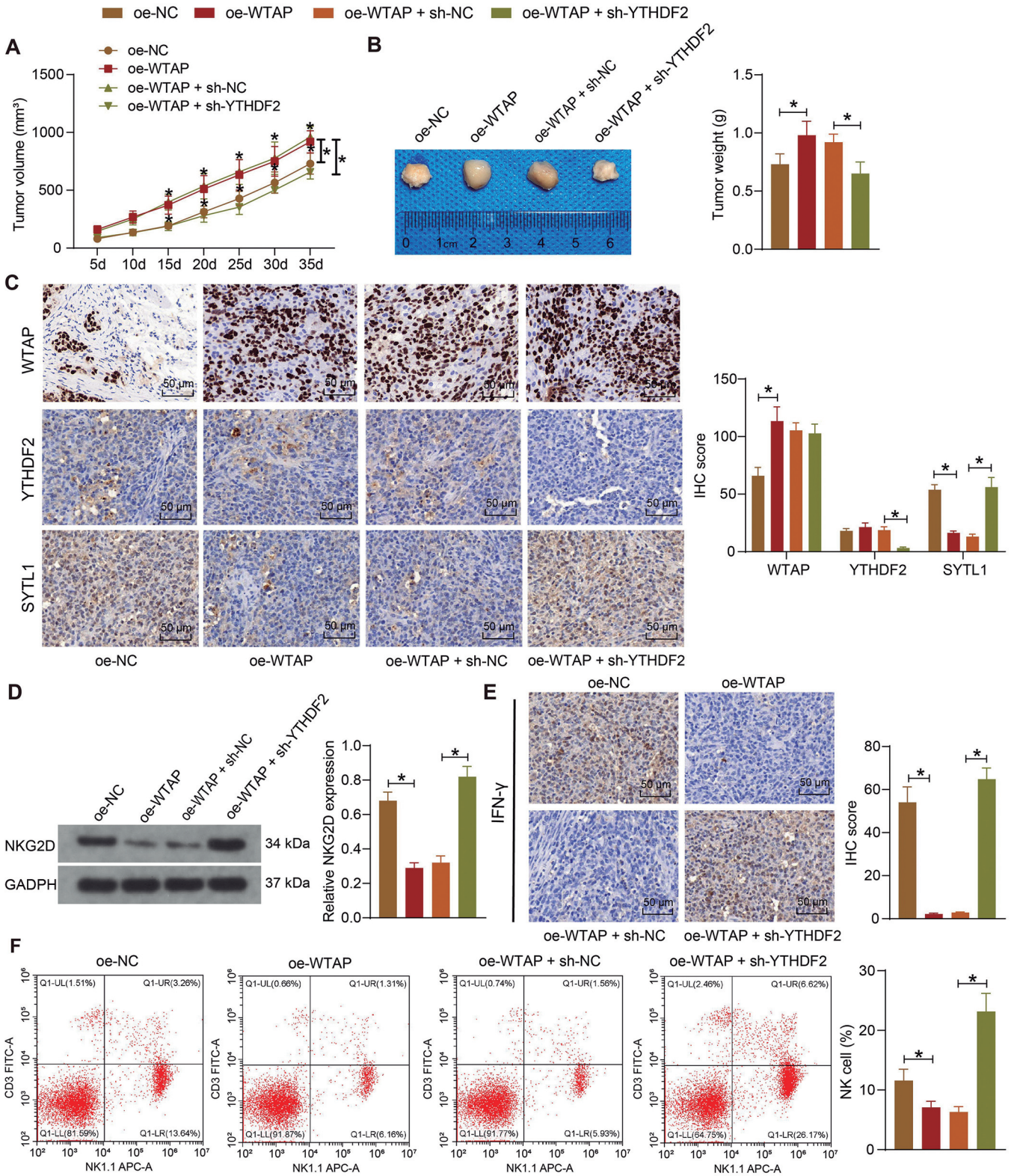

Fig. 6. WTAP and YTHDF2 overexpression in BCa cells mitigate the anti-tumor response of NK cells *in vivo*. 5637 cells infected with oe-WTAP alone or with sh-YTHDF2 (oe-NC or oe-WTAP + sh-NC as controls) were injected into nude mice. **A.** The curve of tumor volume within 35 days. **B.** Representative xenografts and tumor weight detection. **C.** Immunohistochemical detection of WTAP, YTHDF2, and SYTL1 expression in tumor tissues from mice. **D.** NKG2D expression in tumor tissues from mice was measured using western blot assays. **E.** Immunohistochemical detection of IFN-γ expression in tumor tissues from mice. **F.** Flow cytometric detection of NK cells in single cell suspensions isolated from tumor tissues from mice. Data are the mean ± SD (one-way ANOVA (B, D, E, F) or two-way ANOVA (A, C)). n=6 for each group. *p<0.05.

YTHDF2 based on SYTL1 overexpression, and RT-qPCR was performed to detect their expression to verify the efficacy of infection (Fig. 4F). After co-culture with NK-92 cells, the LDH content in the co-culture system was decreased (Fig. 4G), indicating that the lysis of cancer cells by NK-92 cells was inhibited. Moreover, the IFN-γ content (Fig. 4H) and the expression of NKG2D, NKp30, and NKp44 were decreased (Fig. 4I,J), demonstrating that the killing effect of NK-92 cells on SW780 was diminished.

SYTL1 inhibits BCa growth and promotes NK cell-mediated anti-tumor responses in mice

After overexpression of SYTL1 in SW780 cells and subcutaneous injection, a mouse xenograft model was established. Overexpression of SYTL1 slowed tumor growth (Fig. 5A) and reduced tumor weight (Fig. 5B). As the results of immunohistochemistry suggested, SYTL1 expression was overexpressed in the tumor tissues (Fig. 5C). To examine the effects of NK cells *in vivo*, we conducted western blot and immunohistochemistry to measure the expression of NKGD2 and IFN-γ, respectively (Fig. 5D,E). As expected, the expression of these two proteins was enhanced in the tumor tissues of mice injected with oe-SYTL1. Finally, flow cytometry showed an increased number of NK cell activation (Fig. 5F), demonstrating increased NK cell activation and corresponding augmented killing effects.

Silencing of YTHDF2 enhances the anti-tumor response of NK cells in mice in the presence of WTAP overexpression

Mouse xenograft models were established by subcutaneous injection of 5637 cells overexpressing WTAP or simultaneously overexpressing WTAP and silencing YTHDF2. For the measurement of tumor volume and weight, overexpression of WTAP promoted tumor growth (Fig. 6A) and increased tumor weight (Fig. 6B). In contrast, overexpression of WTAP followed by silencing of YTHDF2 inhibited tumor growth (Fig. 6A) and contributed to a decrease in tumor weight (Fig. 6B). Immunohistochemical results showed an increase in WTAP expression and a decrease in SYTL1 expression in tumors extracted from mice expressing WTAP alone, with no significant change in YTHDF2 expression (Fig. 6C). YTHDF2 expression was decreased and SYTL1 expression was elevated in the tumor tissues of mice following the administration of oe-WTAP + sh-YTHDF2 relative to the oe-WTAP + sh-NC administration (Fig. 6C). We then examined NKGD2 and IFN-γ expression in tumor tissues. We found that NKG2D and IFN-γ expression was suppressed in tumors overexpressing WTAP, which was reversed by silencing of YTHDF2 (Fig. 6D,E). Similarly, flow cytometry of cells isolated from tumor tissues showed that the number of activated NK cells was decreased in tumor tissues overexpressing WTAP, while the number of activated NK cells was increased after overexpression of WTAP and silencing of YTHDF2 (Fig. 6F). It was shown that overexpression of WTAP followed by silencing of YTHDF2 enhanced the anti-tumor response of NK cells to BCa cells.

Discussion

m6A RNA modification plays a significant role in the progression of multiple tumorigeneses, and the pan-cancer immune subtype analysis showed the relevance of m6A regulators to the tumor immune microenvironment (Li et al., 2021). Cytotoxic NK cells not only directly kill tumor cells without stimulation by cytotoxic effectors or via death receptor interactions, but also serve as regulatory cells for the immune system by

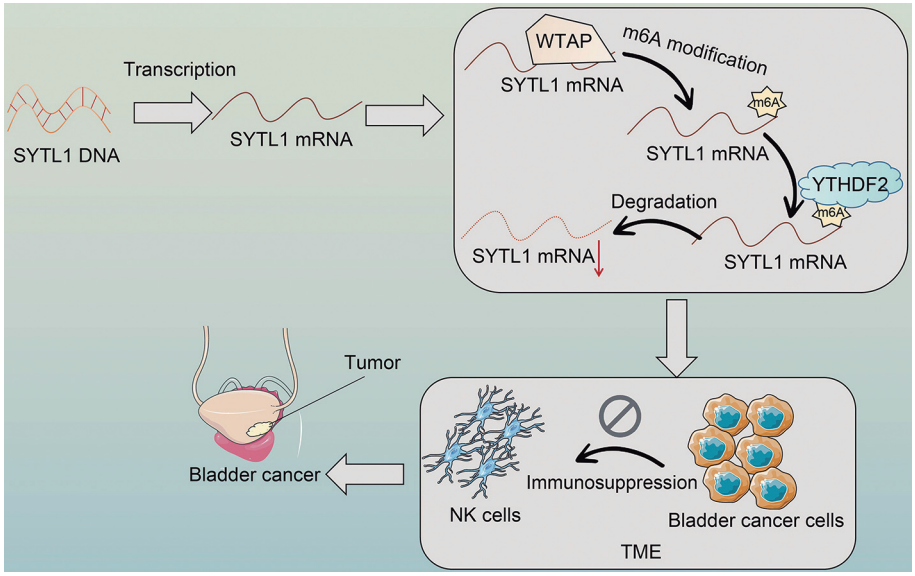

Fig. 7. Proposed model. WTAP inhibits the anti-tumor response of NK cells to BCa cells by promoting YTHDF2 recognition and degradation of SYTL1 mRNA through m6A methylation modification.

secreting cytokines and chemokines (Shevtsov and Multhoff, 2016). In this study, we aimed to demonstrate whether SYTL1 plays a role in BC progression via regulating NK cells. The results showed that SYTL1 was poorly expressed in BC tissues and cells. The upregulation of SYTL1 in BCa cells improved the anti-tumor response of NK cells *in vitro* and *in vivo*. In addition, we observed that the degradation of SYTL1 mRNA in BCa was caused by the m6A methyl-transferase WTAP and the reader protein YTHDF2.

Using Kaplan-Meier Plotter, we not only identified the prognostic value of SYTL1 in BCa but also clarified that this prognostic merit was associated with NK cells. To substantiate the bioinformatics prediction results, we conducted functional assays using a co-culture system. NK cells are cytotoxic lymphocytes of the innate immune system that can kill virally infected and/or cancerous cells, and NK cells-based cancer therapy has currently constituted a major field of immunotherapy innovation (Myers and Miller, 2021). Urologic tumors are infiltrated by NK cells and these NK cells are often dysfunctional (Bhardwaj et al., 2020). NK cells are armed with many activating and inhibitory receptors which can bind to their ligands on target cells, and one of the best-known activating receptors is NKG2D (Del Zotto et al., 2017). There are three activating molecules belonging to natural cytotoxicity receptors: NCR1 (NKp46), NCR2 (NKp44), and NCR3 (NKp30) which are responsible for recognizing tumor cells and inducing cytotoxic effects (Siemaszko et al., 2021). NK cells also produce great quantities of pro-inflammatory cytokines or chemokines such as IFN-γ (Khalil et al., 2021). In the present study, we found that the levels of NKG2D, NKp30, NKp44, and IFN-γ were promoted, which occurred concomitantly with enhanced LDH release, in the supernatant from the co-culture system consisting of NK-92 cells and BCa cells overexpressing SYTL1. Interestingly, hypoxia has been revealed to impair NK cell effector functions (Terren et al., 2019), while SYTL1 was identified as a hypoxia- and immune-associated prognosis signature gene in esophageal squamous cell carcinoma (Lian et al., 2022). Therefore, we hypothesized that the impact of SYTL1 downregulation on NK cell activation was elicited through the hypoxia microenvironment. We will consider further investigation of the specific mechanism of SYTL1 in regulating NK cell activity.

Subsequently, we set to decipher the upstream mechanism of SYTL1 downregulation in BCa. Yokoyama et al. have reported that SYTL1 has been revealed as the MEIS1 target gene in leukemogenesis (Yokoyama et al., 2016). Our team also recently reported that ELK1, a transcription factor, suppressed SYTL1 expression by recruiting HDAC2 in BCa (Wang et al., 2022). In the present study, we turned to m6A modification, an emerging post-transcriptional modification in BCa (Liu, 2021). WTAP was found to be expressed in blood, brain, breast, colorectal, esophagus, eye, head and neck, lung, ovarian, and prostate cancers as well as BCa (Wu et al., 2016). In patients with BCa, high expression of WTAP was associated with poor outcomes, and circ0008399 increased expression of TNFAIP3 by binding to WTAP, thus decreasing BCa cell chemosensitivity to cisplatin (Wei et al., 2021). In this study, we observed that it was WTAP, rather than METTL3, that was negatively correlated with SYTL1 in BCa tissues. The following assays validated that WTAP enhanced the m6A modification of SYTL1 in BCa cells. Further data mining using the GEPIA website showed that YTHDF2 was the reader protein that accelerated the degradation of SYTL1 mRNA.

The overexpression of WTAP and YTHDF2 has been validated in glioblastoma multiforme (Wang et al., 2020) and head and neck squamous cell carcinoma (Paramasivam et al., 2021). Moreover, WTAP was upregulated in nasal-type NK/T-cell lymphoma compared with normal NK cells (Ma et al., 2021). YTHDF2 preferentially recognized m6A and recruited RNA-degrading enzymes to induce rapid degradation of the m6A-containing mRNA (Lee et al., 2020). Consistently, we observed that the degradation of SYTL1 was accelerated in the presence of YTHDF2 in BCa cells. Likewise, the METTL3/YTHDF2 m6A axis directly degraded the SETD7 and KLF4 mRNAs, contributing to BCa development (Xie et al., 2020). To corroborate that WTAP and YTHDF2 were involved in the SYTL1-mediated cytotoxicity by NK cells, we downregulated YTHDF2 expression in 5637 cells with WTAP overexpression or upregulated YTHDF2 expression in SW780 cells with SYTL1 overexpression. We found that YTHDF2 silencing or overexpression overturned the repressive or promoting effects of oe-WTAP or oe-SYTL1 on the NK cell properties both *in vitro* and *in vivo*.

In summary, we demonstrated that SYTL1 overexpression activated NK cells and thereby enhanced anti-tumor immunity *in vitro* and *in vivo*. Additionally, we showed that SYTL1 downregulation was caused by WTAP-mediated m6A methylation and YTHDF2-mediated mRNA degradation (Fig. 7). The findings here support the notion that SYTL1 enhances host anti-tumor immunity and is involved in promoting the therapeutic effects of NK cells.

Funding. This work was supported by the Natural Science Foundation of Hunan Province (No. 2021JJ30403).
Conflict of interest. The authors declare no competing interests.

References

Bhardwaj N., Farkas A.M., Gul Z. and Sfakianos J.P. (2020). Harnessing natural killer cell function for genitourinary cancers. Urol. Clin. North Am. 47, 433-442.

Chen L. and Wang X. (2018). Relationship between the genetic expression of WTAP and bladder cancer and patient prognosis. Oncol. Lett. 16, 6966-6970.

Del Zotto G., Marcenaro E., Vacca P., Sivori S., Pende D., Della Chiesa

M., Moretta F., Ingegnere T., Mingari M.C., Moretta A. and Moretta L. (2017). Markers and function of human NK cells in normal and pathological conditions. Cytometry B Clin. Cytom. 92, 100-114.

Ghandour R., Singla N. and Lotan Y. (2019). Treatment options and outcomes in nonmetastatic muscle invasive bladder cancer. Trends Cancer 5, 426-439.

Grayson M. (2017). Bladder cancer. Nature 551, S33.

He L., Li H., Wu A., Peng Y., Shu G. and Yin G. (2019). Functions of N6-methyladenosine and its role in cancer. Mol. Cancer 18, 176.

Khalil M., Wang D., Hashemi E., Terhune S.S. and Malarkannan S. (2021). Implications of a 'Third Signal' in NK cells. Cells 10, 1955.

Lee Y., Choe J., Park O.H. and Kim Y.K. (2020). Molecular mechanisms driving mRNA degradation by m^6A modification. Trends Genet. 36, 177-188.

Li R., Yin Y.H., Ji X.L., Liu X., Li J.P. and Qu Y.Q. (2021). Pan-cancer prognostic, immunity, stemness, and anticancer drug sensitivity characterization of N6-Methyladenosine RNA modification regulators in human cancers. Front. Mol. Biosci. 8, 644620.

Lian G., Mak T.S., Yu X. and Lan H.Y. (2021). Challenges and recent advances in NK cell-targeted immunotherapies in solid tumors. Int. J. Mol. Sci. 23, 164.

Lian L., Teng S.B., Xia Y.Y., Shen X.M., Zheng Y., Han S.G., Wang W.J., Xu X.F. and Zhou C. (2022). Development and verification of a hypoxia- and immune-associated prognosis signature for esophageal squamous cell carcinoma. J. Gastrointest. Oncol. 13, 462-477.

Liu Q. (2021). Current advances in N6-Methyladenosine methylation modification during bladder cancer. Front. Genet. 12, 825109.

Livak K.J. and Schmittgen T.D. (2001). Analysis of relative gene expression data using real-time quantitative PCR and the $2^{-\Delta\Delta CT}$ method. Methods 25, 402-408.

Ma H., Shen L., Yang H., Gong H., Du X. and Li J. (2021). m6A methyltransferase wilms' tumor 1-associated protein facilitates cell proliferation and cisplatin resistance in NK/T cell lymphoma by regulating dual-specificity phosphatases 6 expression via m6a RNA methylation. IUBMB Life 73, 108-117.

Martinez Rodriguez R.H., Buisan Rueda O. and Ibarz L. (2017). Bladder cancer: Present and future. Med. Clin. (Barc). 149, 449-455.

Meijuan C., Meng X., Fang L. and Qian W. (2023). Synaptotagmin-like protein 1 is a potential diagnostic and prognostic biomarker in endometrial cancer based on bioinformatics and experiments. J. Ovarian Res. 16, 16.

Myers J.A. and Miller J.S. (2021). Exploring the NK cell platform for cancer immunotherapy. Nat. Rev. Clin. Oncol. 18, 85-100.

Paramasivam A., George R. and Priyadharsini J.V. (2021). Genomic and transcriptomic alterations in m6A regulatory genes are associated with tumorigenesis and poor prognosis in head and neck squamous cell carcinoma. Am. J. Cancer Res. 11, 3688-3697.

Shevtsov M. and Multhoff G. (2016). Immunological and translational aspects of NK cell-based antitumor immunotherapies. Front. Immunol. 7, 492.

Siemaszko J., Marzec-Przyszlak A. and Bogunia-Kubik K. (2021). NKG2D natural killer cell receptor-a short description and potential clinical applications. Cells 10, 1420.

Terren I., Orrantia A., Vitalle J., Zenarruzabeitia O. and Borrego F. (2019). NK cell metabolism and tumor microenvironment. Front. Immunol. 10, 2278.

Wang L.C., Chen S.H., Shen X.L., Li D.C., Liu H.Y., Ji Y.L., Li M., Yu K., Yang H., Chen J.J., Qin C.Z., Luo M.M., Lin Q.X. and Lv Q.L. (2020). M6a RNA methylation regulator HNRNPC contributes to tumorigenesis and predicts prognosis in glioblastoma multiforme. Front. Oncol. 10, 536875.

Wang J., Luo J., Wu X. and Li Z. (2022). ELK1 suppresses SYTL1 expression by recruiting HDAC2 in bladder cancer progression. Hum. Cell 35, 1961-1975.

Wei W., Sun J., Zhang H., Xiao X., Huang C., Wang L., Zhong H., Jiang Y., Zhang X. and Jiang G. (2021). *Circ0008399* interaction with WTAP promotes assembly and activity of the m6A methyltransferase complex and promotes cisplatin resistance in bladder cancer. Cancer Res. 81, 6142-6156.

Wu L.S., Qian J.Y., Wang M. and Yang H. (2016). Identifying the role of wilms tumor 1 associated protein in cancer prediction using integrative genomic analyses. Mol. Med. Rep. 14, 2823-2831.

Xie H., Li J., Ying Y., Yan H., Jin K., Ma X., He L., Xu X., Liu B., Wang X., Zheng X. and Xie L. (2020). METTL3/YTHDF2 m^6 a axis promotes tumorigenesis by degrading SETD7 and KLF4 mRNAs in bladder cancer. J. Cell Mol. Med. 24, 4092-4104.

Xu X., Wang Y., Zhang S., Zhu Y. and Wang J. (2021). Exploration of prognostic biomarkers of muscle-invasive bladder cancer (MIBC) by bioinformatics. Evol. Bioinform. Online 17, 11769343211049270.

Yokoyama T., Nakatake M., Kuwata T., Couzinet A., Goitsuka R., Tsutsumi S., Aburatani H., Valk P.J., Delwel R. and Nakamura T. (2016). MEIS1-mediated transactivation of synaptotagmin-like 1 promotes CXCL12/CXCR4 signaling and leukemogenesis. J. Clin. Invest. 126, 1664-1678.

Zhao H., Xu Y., Xie Y., Zhang L., Gao M., Li S. and Wang F. (2021). m6A regulators is differently expressed and correlated with immune response of esophageal cancer. Front. Cell Dev. Biol. 9, 650023.

Accepted October 23, 2023